Similarities and Differences in the Supramolecular Organization of Silkworm and Spider Silk

José Pérez-Rigueiro, Manuel Elices,* Gustavo R. Plaza, and Gustavo V. Guinea

Departamento de Ciencia de Materiales, ETSI Caminos, Canales y Puertos, Universidad Politécnica de Madrid, 28040 Madrid, Spain

Received February 26, 2007; Revised Manuscript Received May 22, 2007

ABSTRACT: The characterization of silkworm and spider silk from nanometer to micrometer scale by atomic force microscopy reveals similar design principles despite the distance of their spinning organisms in evolutionary terms. Nanoglobules are the basic microstructural blocks in both materials, but this common microstructural design is tuned to fulfill the biological function of each silk. Spider silk nanoglobules are isotropic, and its size varies during stretching. Silkworm silk nanoglobules are anisotropic and loosely aligned with the fiber axis. The combination of our results with previous data on the structure of silks at a molecular level allows a model of the supramolecular organization of both silkworm and spider silk to be proposed. The detailed characterization of the microstructure of natural silks should contribute to the development and production of a new family of bioinspired fibers.

1. Introduction

Silks spun by arthropods constitute a group of materials with exceptional mechanical properties,[1] which are expected to be the basis of a new family of high-performance artificial fibers.[2] The exceptional properties of silks are firmly based on protein sequences, whose exquisite adaptation to their function is indicated by the conservation of their main motifs in related species for hundreds of millions of years[3,4] and by the homologies in the sequence of silk proteins which surged from independent evolutionary events.[5] Thus, it has been found that the sequences of both silkworm silk and major ampullate gland spider silk (MAS) proteins show repeating motifs that, albeit different, share the ability to form β-microcrystallites.[6,7]

Silkworm silk is made up of a core composed of two proteins of the fibroin family and by a coating composed of proteins of the sericin family. The fibroins of the core are labeled as heavy chain and light chain according to their molecular weights, and it is assumed that the heavy chain is responsible for the mechanical properties of the core and of the fiber as a whole.[1] The sericin coating acts as a glue and maintains the structural integrity of the cocoon but makes a negligible contribution to its mechanical properties.

The entire sequence of fibroin is known.[8] Fibroin heavy chain shows frequent repetitions of the motif −GAGAGS− that form β microcrystallites in the fiber.[6] The size of the β microcrystallites has been determined by X-ray diffraction, and a value of 21 nm × 6 nm × 2 nm has been reported.[9] The microstructural characterization at the submicron scale has yielded evidence of a nanofibrilar structure,[10−12] although the inner organization of the nanofibrils has not been described.

In contrast to silkworm silk, the biological function of the silk produced by the major ampullate gland of spiders (MAS) in the structure of the web and as a safety line does not require a high elastic modulus but depends on its ability to sustain large strains at high stresses and to dissipate most of the mechanical energy required for its deformation. Precisely, the combination of tensile strength and strain at breaking endows MAS with the highest work of fracture of any material, either natural or artificial. The only microstructural detail of spider silk that has been firmly established is the presence of β microcrystallites[7] at the molecular level. Some studies have proposed a nanofibrilar microstructure for MAS, mainly from low-resolution AFM observations,[10,13,14] but this hypothesis has been disputed by experimental results obtained with other techniques.[15,16]

From the point of view of its composition, MAS shows significant differences when compared to silkworm silk. In this respect, MAS is composed of two proteins:[3] spidroin 1 and spidroin 2, and both proteins are believed to contribute to the mechanical properties of the fiber. Spidroin 1 presents three main motifs frequently repeated along its sequence: polialanine runs, A_n ($n = 5-8$), GGX motifs (X = Q, L, or Y), and GA motifs. Spidroin 2 also presents three motifs: polialanine runs, GGX motifs, and GPG motifs. Polialanine runs and GGX motifs are found in both proteins, although the latter is rarer in spidroin 2. The polialanine runs of both proteins pile up to form β microcrystallites.

The mechanical behavior of MAS also differs from that of silkworm silk: MAS is more compliant and can sustain repeated cycles of stretching and recovery.[17] Recovery of irreversibly stretched MAS depends on the supercontraction effect,[18] a reduction of the length of the fiber down to 50% of its initial length when unrestrained and submerged in water. The supercontraction effect has been used to develop techniques to modify the tensile properties of MAS fibers in a controlled, reproducible, and reversible way.[19] Such procedures are based on the dependence of the tensile properties on the alignment of the silk proteins. The two extreme states of alignment in MAS fibers are labeled conventionally as forcibly silked (FS; corresponding to maximum alignment) and after maximum supercontraction (MS; corresponding to minimum alignment).[20]

Despite the identification of the β microcrystallites at the molecular level, the task of identifying the microstructural organization at the nanometer scale has remained elusive, although it is a critical step to understand the relationship between the sequence and the macroscopic properties of silk, and it should allow to guide the spinning of artificial fibers bioinspired in natural silks. We have used atomic force microscopy to obtain high-resolution images of spider and

* Corresponding author. E-mail: melices@mater.upm.es.

10.1021/ma070478o CCC: $37.00
Published on Web 06/26/2007

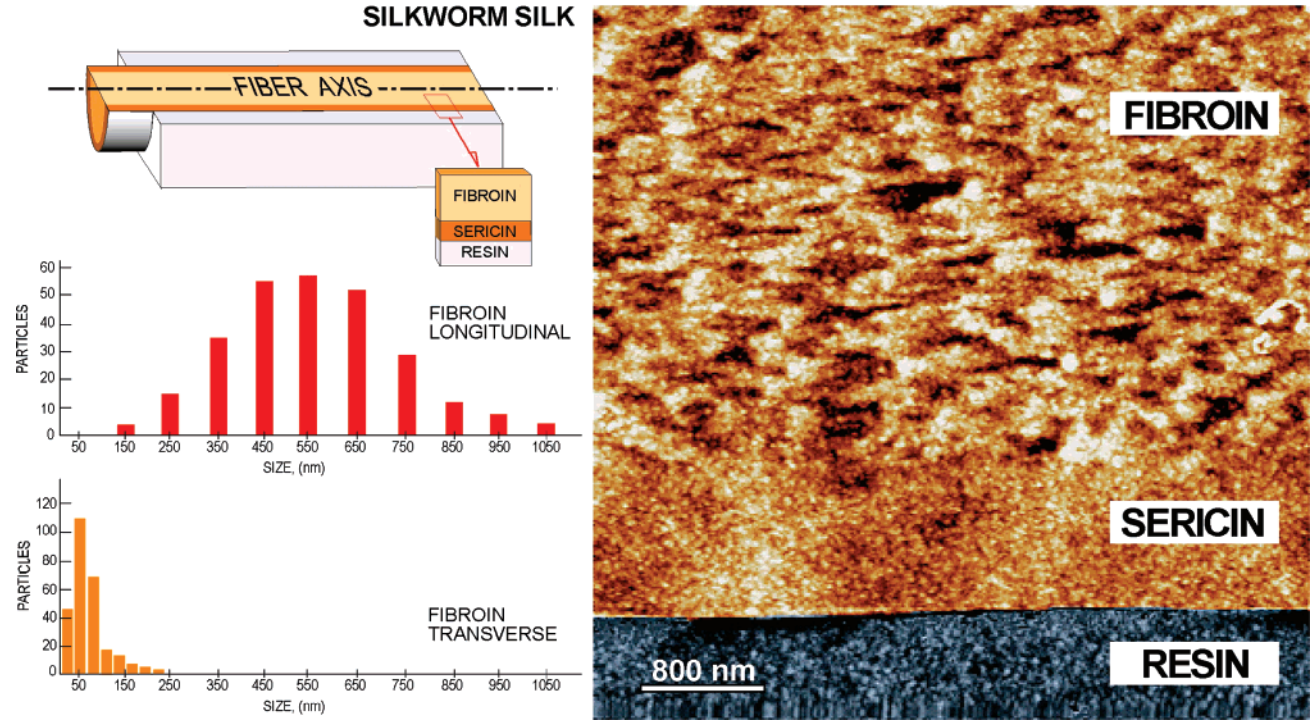

Figure 1. AFM image (4 μm × 4 μm) of the longitudinal section of a silkworm silk (*Bombyx mori*) silk fiber showing the fibroin core and the sericin coating. The macroscopic axis of the fiber lies along the horizontal axis of the image as shown in the scheme chart. The sizes of the elongated microstructural details in the longitudinal (parallel to the fiber's axis) and transverse (perpendicular to fiber's axis) directions are shown as histograms. Their mean values ± standard deviation are 600 ± 200 nm (longitudinal direction) and 90 ± 30 nm (transverse direction).

silkworm silk from the nanometer scale to the micrometer scale for the first time. It has been found that, despite the differences in both sequence and evolutionary origin, both materials share a common nanoglobular organization, which is adapted to the expected biological function of each silk: a stiff fiber that protects the pupa during metamorphosis[21] (silkworm, *Bombyx mori*, silk) and a fiber that sustains large strains and dissipates most of the mechanical energy used in its deformation as required by its function in the web and as a lifeline[22] (spider silk).

2. Experimental Section

Silkworm silk fibers were retrieved by forced silking.[23] *B. mori* silkworms were reared to the fifth larval stage on a diet of mulberry leaves. Immediately after they stopped feeding, they were subjected to constant surveillance to detect the onset of cocoon spinning. When silk was first observed, the worm was placed on a black surface and allowed to spin a short length of fiber. The spun fiber was grasped with tweezers and reeled from the worm by hand at a nominal speed of 1 cm/s.

Argiope trifasciata (Argiopidae) MAS fibers were retrieved by forced silking[24,25] (FS fibers). Spiders were immobilized in a self-zipping bag, in which a hole has been perforated to make the spinneret accessible. The silk is reeled on a polyethylene mandrel that combines simultaneous rotation and translation around and along its axis. Forced silking process proceeded at 20 mm/s.

MS fibers were prepared from FS fibers through a maximum supercontraction process.[20] FS fibers were glued on perforated aluminum foil frames by their ends. The gauge length of the samples before maximum supercontraction was measured by reckoning the maximum length between the glued ends of the fiber with no force exerted on the fiber. Maximum supercontraction was attained in the following way: The gauge length was decreased down to a 40% of the initial gauge length, and then samples were immersed in water for 30 min and allowed to dry overnight (nominal conditions T = 20 °C, relative humidity 35%). The gauge length of the samples after maximum supercontraction was measured by reckoning the maximum length between the glued ends of the fiber with no force exerted on the fiber.

Fibers from at least two different specimens of each species were used in this study. Fibers were stained with Richardson methylene blue to facilitate cutting, since the low contrast between the fiber and the embedding resin in the optical microscope represents a major difficulty during the preparation of longitudinal samples by ultramicrotomy. Staining proceeded by covering the fiber with a drop of methylene blue, heating at 60 °C, and washing gently with water when the drop was observed to dry. The fiber was kept taut and their ends secured during staining, since it has been found that the properties of silk fibers are not affected by immersion in water and subsequent drying under these conditions.[20] Stained fibers were embedded in Spurr's resin and allowed to cure for 72 h at 70 °C. The function of Spurr's resin is to serve as mechanical support to the fiber during the ultramicrotomy step. The low infiltration ability of small organic molecules such as ethanol and acetone into silk[26] further suggests that the resin does not penetrate in the fiber and, consequently, does not modify the microstructure of the fiber. The longitudinal sections were obtained by ultramicrotomy with a diamond blade.

A Bermad 2000 AFM (Nanotec Electrónica, Spain) was used to record the atomic force microscopy images. Olympus OMCL RC800PSA (Si_3N_4; tip radius <20 nm) cantilevers were used for the observation, and the highest resolution was obtained with the stiffest tip (100 μm × 40 μm; nominal stiffness 0.76 N/m). AFM images were obtained in the dynamic mode in the repulsive regime of the tip−sample interaction, since it has been found that this regime allows reaching the highest resolution.[27] Observation in the repulsive regime requires low values of the amplitude of the tip oscillation (typically ≈0.020 V). Images were obtained at a frequency of 1 Hz in the low scan direction (Y-direction). At least two samples of each material and condition were observed, and each sample was observed with at least two different AFM tips. A gallery of images from different samples and at different scales is presented as Supporting Information.

The processing of AFM images has consisted of simply equalizing and adjusting the contrast and the brightness of the micro-

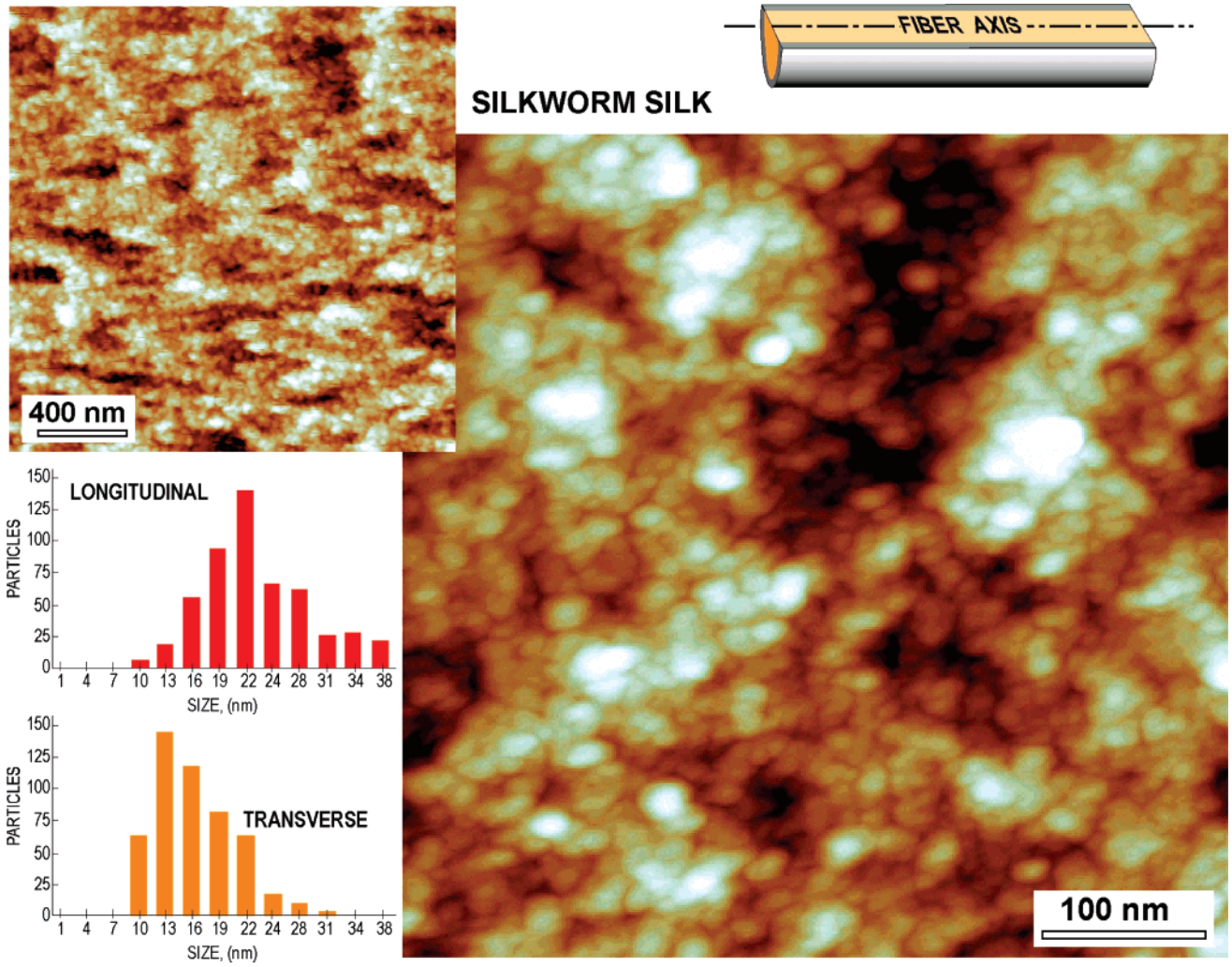

Figure 2. AFM image (500 nm × 500 nm) of the longitudinal section of a silkworm silk (*Bombyx mori*) fiber. The macroscopic axis of the fiber lies along the horizontal axis of the image as shown in the scheme chart. The distribution of the size of the nanoglobules in the longitudinal (parallel to the fiber's axis) and transverse (perpendicular to fiber's axis) are shown as histograms. The mean values ± standard deviation of the size of the nanoglobules are 23 ± 6 nm (longitudinal) and 16 ± 4 nm (transverse). A 2 μm × 2 μm AFM image shows again the elongated microstructural details at micrometer scale observed in Figure 1.

graphs. No filter has been used to improve the quality of the images or to highlight their details. In particular, the effect of tip dilation[28] has not been used to recalculate the dimensions of the microstructural features. However, the observation of microstructural details with lateral dimensions of ~7 nm sets an upper limit to the extent of the convolution between tip and sample. A lower limit of 7−8 nm has also been established from the observation of biomolecules of known lateral dimensions, such as DNA and polylysine. The size of AFM tips usually ranges from 5 to 20 nm depending on the manufacturer and on the use of sharpening techniques,[29,30] in excellent agreement with the resolution of our AFM images. Besides, since all the discussion is based on experimental details which are at least 50% larger than this lower limit, the conclusions remain unaffected by this limitation on the resolution of the AFM images.

3. Results and Discussion

Figure 1 shows a longitudinal section of a silkworm silk fiber. The differences between the fibroin core, the sericin coating, and the resin, in which the fiber is embedded, are evident. Longitudinal microstructural details are found in the fibroin core with a mean length of 600 nm and a mean width of 90 nm, although some details are shown to reach a length of 1000 nm. Previous works[10−12] have shown lower resolution images with microstructural details identified as nanofibrils with longitudinal dimensions in the range 1000−2000 nm[12] and with transverse dimensions[10−12] in the range from 80 to 400 nm, with an average transverse dimension of 140 nm. These values compare well with the dimension of the longitudinal features observed in Figure 1.

High-resolution images of the fibroin core have allowed identifying the structure of the fibroin core at a nanometer scale (Figure 2). It has been found that the fibroin core consists of nanoglobules, whose distribution of sizes is shown in the histograms in Figure 2. Silkworm silk nanoglobules are anisotropic with a mean length of 23 nm along the fiber axis and a mean width of 16 nm perpendicular to the fiber axis. Comparable nanoglobules have been found in fibroin aggregates adsorbed on monocrystalline silicon.[31] The similarity between the size of the β microcrystallites as measured by X-ray diffraction (21 nm × 6 nm × 2 nm) and that of the nanoglobules observed by AFM immediately suggests that each nanoglobule consists essentially of a β microcrystallite. This model implies that each β microcrystallite must be surrounded by a less ordered region, as required by the existence of an amorphous phase that represents ~50% of the volume of the fiber.[32,33]

The comparison of the observations at micrometer and nanometer scales (Figures 1 and 2) shows that the nanoglobules

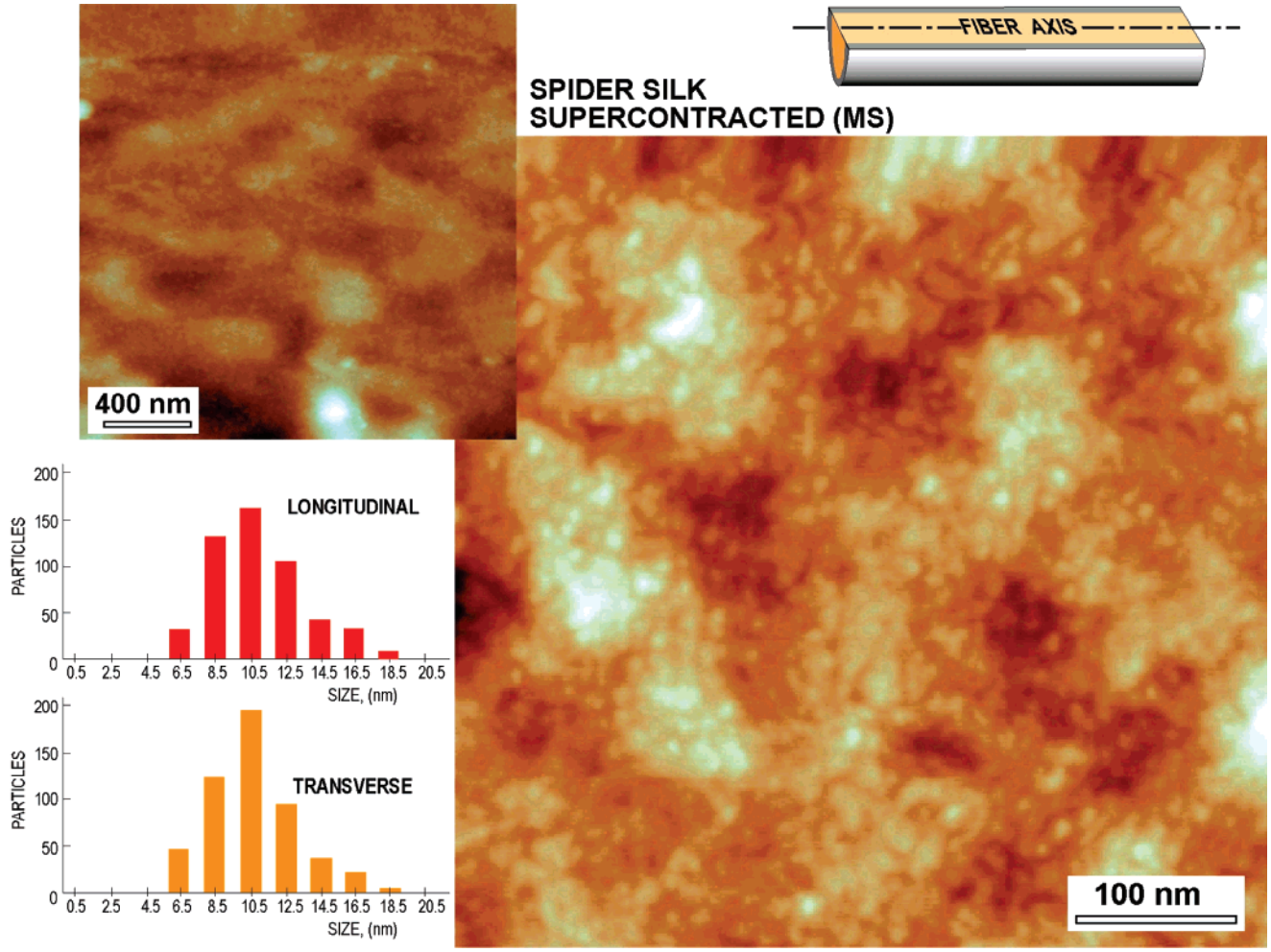

Figure 3. AFM image (500 nm × 500 nm) of the longitudinal section of a spider silk (MAS; *Argiope trifasciata*) fiber in the maximum supercontracted (MS) state, corresponding to the minimum alignment of the protein chains. The macroscopic axis of the fiber lies along the horizontal axis of the image as shown in the scheme. The distribution of the size of the nanoglobules in the longitudinal (parallel to the fiber's axis) and transverse (perpendicular to the fiber's axis) are shown as histograms. The mean values ± standard deviation of the size of the nanoglobules are 10 ± 2 nm, both in the longitudinal and transverse directions. A 2 μm × 2 μm AFM image is also shown, and no additional structural details at the micrometer scale are observed.

are loosely associated, so that this association is not apparent at the nanometer scale. Although the longitudinal microstructural details at micrometer scale have been usually referred to as nanofibrils, Figure 2 shows that their structure does not correspond to the succession of oriented regions aligned along the fiber's macroscopic axis, which defines a fibrilar microstructure.[34] The difference in the microstructural details found at different observation scales is probably the result of significant local deviations of the protein chain from the macroscopic axis of the fiber but reflects the average alignment of the chains at larger scales. A loose alignment of the chains allows the combination of a relatively high elastic modulus with the ability of sustaining large strains at breaking. A more perfect alignment of the chains along the macroscopic axis of the fiber leads to stiff polymers with low strain at breaking.[35]

MAS fibers in the FS and MS states have been observed by AFM to characterize the influence of the molecular alignment on the features of the microstructure from the nanometer scale to the micrometer scale. Figures 3 and 4 show AFM images of longitudinal sections of MAS fibers corresponding to MS and FS states, respectively. Despite the differences in the tensile properties exhibited by FS and MS fibers,[20] both samples share a nanoglobular microstructure formed by isotropic nanoglobules with comparable sizes in the directions parallel and perpendicular to the macroscopic axis of the fiber. No other microstructural detail is apparent up to the micrometer scale, so that no evidence supporting the presence of nanofibrils in MAS fibers has been found, despite the transverse dimension of the proposed nanofibrils ranges from 60 nm[14] to 150 nm[13] well above the microstructural details presented in this work.

However, there are significant differences in the size of the nanoglobules exhibited in both states. The sizes of the nanoglobules of the MS state show a distribution with a mean value of 10 nm (standard deviation 2 nm) and a maximum size of 17 nm. In contrast, the nanoglobules of the FS state appear to show a distribution with a mean value of 13 nm (standard deviation 4 nm). The maximum size of the nanoglobules in the FS state is 22 nm. Studies on the morphology of artificial proteins constructed from the sequence of MAS[36] have allowed globular aggregates to be identified, although the size of the aggregates is larger (40 nm) than the size of the nanoglobules of either MS or FS states.

The presence of β microcrystallites formed by polialanine runs, which are not affected by the supercontraction effect[37] except for their orientation relative to the macroscopic axis of the fiber, is compatible with the size of the nanoglobules of the MS state, especially if it considered that the convolution between tip and sample likely leads to a certain increase in the size of the nanoglobules as observed by AFM. The calculation of the distance between the C_α of the two extreme polialanines in a

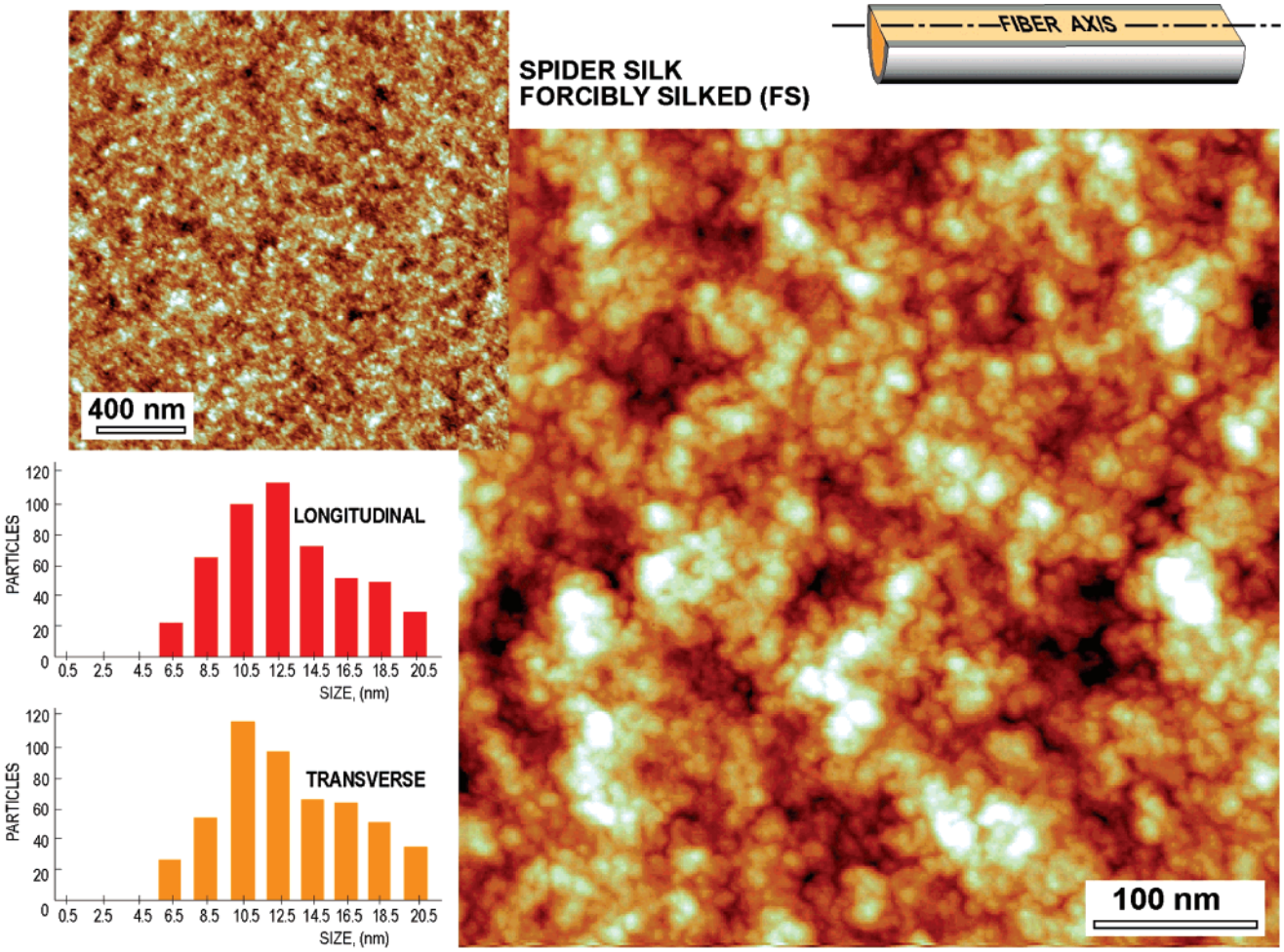

Figure 4. AFM image (500 nm × 500 nm) of the longitudinal section of a spider silk (MAS; *Argiope trifasciata*) fiber in the forcibly silked (FS) state, corresponding to the maximum alignment of the protein chains. The macroscopic axis of the fiber lies along the horizontal axis of the image as shown in the scheme. The distribution of the size of the nanoglobules in the longitudinal (parallel to the fiber's axis) and transverse (perpendicular to fiber's axis) are shown as histograms. The mean value ± standard deviation of the nanoglobules is 13 ± 4 nm, both in the longitudinal and transverse directions. A 2 μm × 2 μm AFM image is also shown, and no additional structural details at the micrometer scale are observed.

polialanine run A_8 from the theoretical bond lengths and angles in a β sheet yields a value of 2.9 nm. This value correlates well with the size of microcrystallites as determined by X-ray diffraction, which is found to be 2−3 nm.[7] Consequently, it is reasonable to assume that each nanoglobule consists of a β microcrystallite surrounded by less ordered regions from both spidroins. This interpretation is consistent with the fraction of crystalline regions in MAS fibers, which represents at most 40% of the total mass of the fiber.[32,33]

Since the reversible interconversion of the MS and FS states does not modify the β microcrystals of polialanine, except for variations in the alignment of the microcrystals with the macroscopic axis of the fiber, the explanation for the increase of the size of the nanoglobules must be found in other motifs of the protein sequence. Thus, its has been proposed that the GGX and GA motifs interspersed between the polialanine runs may align to form nonperiodic lattices (NPL).[38] NPLs are defined by the probabilistic character of the periodicity of their constituent elements, in contrast with the deterministic character of the periodicity in true crystals. Such an explanation is also consistent with the intermolecular distances calculated from the sequence, since the theoretical length of the region between two consecutive polialanine runs in spidroin 1 is 12 nm, if a β pleated secondary structure is assumed. This hypothesis is also supported by the significant increase in the mobility of GGX motifs observed in supercontracted silk,[39] which is consistent with the disorganization of the NPLs during the supercontraction process. Disorganization of NPLs would be a reversible process that can be reverted by stretching the fiber submerged in water.[19,40] In this context, the process of formation of NPLs constitutes a likely mechanism of energy dissipation during stretching of spider silk fibers.

4. Conclusions

The detailed microstructural characterization of silkworm and spider silk from the nanometer to the micrometer scale has revealed that nanoglobules are common microstructural features shared by both materials. Nanoglobules are loosely aligned with the fiber axis in silkworm silk, but no proper nanofibrilar organization is observed. No alignment has been found in the nanoglobules of spider silk fibers. It has been found that the size of the nanoglobules in spider silk increases when the fiber is subjected to stretching, suggesting a possible mechanism that explains the ability of spider silk to dissipate energy. The characterization of the similarities and differences in the microstructures of silkworm and spider silk at nanometer scale opens new possibilities for understanding and modeling silks. In particular, it suggests that efforts to create new bioinspired fibers of properties comparable to natural silks should be directed to reproduce the highly conserved nanoglobular microstructure observed in both silkworm and spider silk.

Acknowledgment. *A. trifasciata* spiders were provided and reared by O. Campos (ReptilMadrid, Madrid, Spain). Ultramicrotomy was performed by E. Baldonedo (Centro de Microscopía Electrónica, Universidad Complutense de Madrid, Spain). J.M. Martínez helped in the preparation of the figures. The authors thank Dr. A. Gil (Nanotec Electrónica S.L., Madrid, Spain) for her technical support. This work was funded by Ministerio de Educación y Ciencia (Spain) (MAT 2006-04387) and by Comunidad de Madrid (Spain) (ESTRUMAT-CM: MAT/77).

Supporting Information Available: Images from different samples and at different scales of maximum supercontraction, forced silking, and silkworm silk. This material is available free of charge via the Internet at http://pubs.acs.org.

References and Notes

(1) Kaplan, D. L.; Lombardi, S. L.; Muller, W. S.; Fossey, S. A. In *Biomaterials: Novel Materials from Biological Sources*; Byrom, D., Ed.; Stockton Press: New York, 1991; pp 1−53.
(2) Lazaris, A.; Arcidiacono, S.; Huang, Y.; Zhou, J.-F.; Duguay, F.; Chretien, N.; Welsh, E. A.; Soares, J. W.; Karatzas, C. N. *Science* **2002**, *295*, 472−476.
(3) Gatesy, J.; Hayashi, C.; Motriuk, D.; Woods, J.; Lewis, R. *Science* **2003**, *291*, 2603−2605.
(4) Garb, J. E.; DiMauro, T.; Vo, V.; Hayashi, C. Y. *Science* **2006**, *312*, 1762.
(5) Craig, C. L. *Annu. Rev. Entomol.* **1997**, *42*, 231−267.
(6) Marsh, R. B.; Corey, L.; Pauling, L. *Biochim. Biophys. Acta* **1955**, *16*, 1−34.
(7) Work, R. W.; Morosoff, N. *Textile Res. J.* **1982**, *52*, 349−356.
(8) Xia, Q.; et al. *Science* **2004**, *306*, 1937−1940.
(9) Fraser, R. B. C.; MacRae, T. P. *Conformation in Fibrous Proteins*; Academic Press: New York, 1973; pp 293−343.
(10) Miller, L. D.; Putthanarat, S.; Eby, R. K.; Adams, W. W. *Int. J. Biol. Macromol.* **1999**, *24*, 159−165.
(11) Putthanarat, S.; Stribeck, N.; Fossey, S. A.; Eby, R. K.; Adams, W. W. *Polymer* **2000**, *41*, 7735−7747.
(12) Poza, P.; Pérez-Rigueiro, J.; Elices, M.; Llorca, J. *Eng. Fract. Mech.* **2002**, *69*, 1035−1048.
(13) Li, S. F. Y.; McGhie, A. J.; Tang, S. L. *Biophys. J.* **1994**, *66*, 1209−1212.
(14) Du, N.; Liu, X. Y.; Narayanan, J.; Li, L.; Lim, M. L. M.; Li, D. *Biophys. J.* **2006**, *91*, 4528−4535.
(15) Glisovic, A.; Thieme, J.; Guttmann, P.; Salditt, T. *Int. J. Biol. Macromol.* **2007**, *40*, 87−95.
(16) Mahoney, D. V.; Vezie, D. L.; Eby, R. K.; Adams, W. W.; Kaplan, D. In *Silk Polymers. Materials Science and Biotechnology*; Kaplan, D., Adams, W. W., Farmer, B., Viney, C., Eds.; American Chemical Society: Washington, DC, 1994; pp 196−210.
(17) Elices, M.; Pérez-Rigueiro, J.; Plaza, G.; Guinea, G. V. *J. Appl. Polym. Sci.* **2004**, *92*, 3537−3541.
(18) Work, R. W. *Textile Res. J.* **1977**, *47*, 650−662.
(19) Guinea, G. V.; Elices, M.; Pérez-Rigueiro, J.; Plaza, G. R. *J. Exp. Biol.* **2005**, *208*, 25−30.
(20) Pérez-Rigueiro, J.; Elices, M.; Guinea, G. V. *Polymer* **2003**, *44*, 3733−3736.
(21) Asakura, T.; Kaplan, D. L. *Encycl. Agric. Sci.* **1994**, *4*, 1−11.
(22) Vollrath, F. *Sci. Am.* **1992**, *266*, 70−76.
(23) Pérez-Rigueiro, J.; Elices, M.; Llorca, J.; Viney, C. *J. Appl. Polym. Sci.* **2001**, *82*, 1928−1935.
(24) Work, R. W.; Emerson, P. D. *J. Arachnol.* **1982**, *10*, 1−10.
(25) Guinea, G. V.; Elices, M.; Real, J. I.; Gutiérrez, S.; Pérez-Rigueiro, J. *J. Exp. Zool. A* **2005**, *303*, 37−44.
(26) Pérez-Rigueiro, J.; Viney, C.; Llorca, J.; Elices, M. *Polymer* **2000**, *41*, 8433−8439.
(27) García, R.; San Paulo, A. *Phys. Rev. B* **1999**, *60*, 4961−4967.
(28) Morris, V. J.; Kirby, A. R.; Gunning, A. P. *Atomic Force Microscopy for Biologists*; Imperial College Press: London, UK, 1999; p 32.
(29) Lüthi, R.; Meyer, E.; Bammerlin, M.; Baratoff, A.; Lü, J.; Guggisberg, M.; Güntherodt, H.-J. In *Scanning Probe Microscopy in Polymers*; Ratner, B. D., Tsukruk, V. V., Eds.; American Chemical Society: Washington, DC, 1998; pp 300−311.
(30) Sheiko, S. S. In *New Developments in Polymer Analytics II*; Adv. Polym. Sci. 151; Schmidt, H., Ed.; Springer-Verlag: Berlin, 2000; pp 61−174.
(31) Shulha, H.; Wong Po Foo, C.; Kaplan, D. L.; Tsukruk, V. V. *Polymer* **2006**, *47*, 5821−5830.
(32) Gillespie, D. B.; Viney, C.; Yager, P. In *Silk Polymers. Materials Science and Biotechnology*; Kaplan, D., Adams, W. W., Farmer, B., Viney, C., Eds.; American Chemical Society: Washington, DC, 1994; pp 155−167.
(33) Lefèvre, T.; Rousseau, M.-E.; Pézolet, M. *Biophys. J.*, doi:10.1529/biophysj.106.100339.
(34) Warner, S. B. *Fiber Science*; Prentice Hall: Englewood Cliffs, NJ, 1995; pp 30−67.
(35) Chawla, K. K. *Fibrous Materials*; Cambridge University Press: Cambridge, 1992; pp 58−107.
(36) Oroudjev, E.; Soares, J.; Arcidiacono, S.; Thompson, J. B.; Fossey, S. A.; Hansma, H. G. *Proc. Natl. Acad. Sci. U.S.A.* **2002**, *99*, 6406−6465.
(37) Simmons, A. H.; Michal, C. A.; Jelinski, L. W. *Science* **1996**, *271*, 84−87.
(38) Viney, C. In *Structural Biological Materials*; Elices, M., Ed.; Pergamon Press: Amsterdam, 2000; pp 293−333.
(39) Yang, Z.; Liivak, O.; Seidel, A.; LaVerde, G.; Zax, D. B.; Jelinski, L. W. *J. Am. Chem. Soc.* **2000**, *122*, 9019−9025.
(40) Plaza, G. R.; Guinea, G. V.; Pérez-Rigueiro, J.; Elices, M. *J. Polym. Sci., Part B: Polym. Phys.* **2006**, *44*, 994−999.

MA070478O